An Impedance Matched Phase Shifter Using $\mathrm{BaSrTiO_3}$ Thin Film

Qingduan Meng, Xueqiang Zhang, Fei Li, Jiandong Huang, Xiaohong Zhu, Dongning Zheng, Bolin Cheng, Qiang Luo, Changzhi Gu, and Yusheng He

***Abstract*—We present a distributed phase shifter with an equal ripple return loss at its operation frequency range. The phase shifter is based on a periodic structure and consists of a coplanar waveguide (CPW) line periodically loaded with voltage-variable barium strontium titanate (BST) interdigitated capacitors. Measurements show that its return loss is better than −15 dB at frequencies from direct current to 16 GHz, and at 9.4 GHz, its phase shift is 41° under 120-V applied bias voltage.**

***Index Terms*—$\mathbf{Ba_{1-x}Sr_xTiO_3}$ (BST), distributed circuits, phase shifter.**

I. INTRODUCTION

AT THE present time, the phase array antennas are being increasingly used for X-band communication and radar systems [1]. Generally, the phase array antennas need a large number of phase shifters. Phase shifters using $\mathrm{Ba_{1-x}Sr_xTiO_3}$ (BST) thin films have been widely investigated, which is a promising component for applications in phase array antennas, and its main advantages are higher tunability, faster operation speed, increased microwave power, lower cost, and smaller size. Several groups [2]–[5] have implemented phase shifters using BST thin films which are based on single periodic structures. Among these applications [3]–[5], either interdigital or parallel plate capacitors are used for loading the transmission lines with spacing L_{sect}. In these phase shifters, well below the Bragg frequency, their return losses always increase with increasing frequency. In order to improve the performance of the phase shifter, in this letter, a new periodic structure was suggested, which improves the impedance matching of the circuits. Thus, in the whole operation frequency range, the local return loss maxima of the phase shifter appear at more or less the same level, simultaneously its operation frequency range is broadened. A demonstration X-Band phase shifter has been designed and fabricated using this new structure.

II. BASIC THEORIES FOR NEW PERIODIC STRUCTURE

In the single periodic structure employed in [6], BST capacitors are periodically placed with spacing L_{sect}. The Bragg frequency can be estimated by the lumped element model [6] as

$$f_{\mathrm{Bragg}} = \frac{1}{\pi\sqrt{L_l\left[C_l + C_{\mathrm{BST}}(V)\right]}} \tag{1}$$

where L_l and C_l are the high-impedance line section inductance and capacitance, respectively, and $C_{\mathrm{BST}}(V)$ is voltage variable BST capacitance. At certain given frequency, the possible maximum differential phase shift obtainable from a single section is given by

$$\delta\phi = 2\pi f\frac{L_{\mathrm{sec}\,t}}{\nu_i}\left(\sqrt{1+x} - \sqrt{1+xy}\right) \tag{2}$$

where ν_i is the phase velocity of a wave on the high-impedance line and given by

$$\nu_i = \frac{L_{\mathrm{sec}\,t}}{\sqrt{L_l\left[C_l + C_{\mathrm{BST}}(V)\right]}} \tag{3}$$

In (2), x is the loading factor and y is the capacitance ratio, which are defined as follows, respectively:

$$x = \frac{C_{\mathrm{BST}}^{\max}/L_{\mathrm{sec}\,t}}{C_l} \tag{4}$$

$$y = \frac{C_{\mathrm{BST}}^{\min}}{C_{\mathrm{BST}}^{\max}} \tag{5}$$

here the parameter y is the ratio of the minimum-to-maximum BST capacitance, which is only determined by the external bias electric field. The larger external applied bias voltage is, the smaller BST capacitor becomes, the more obtained differential phase will be. The loading factor (x) is the ratio of maximum BST capacitance per unit length to the transmission line capacitance per unit length.

Comparing with the single periodic structure, the only altered parameter in this proposed new periodic structure is the loading spacing, and all the others, such as BST material and capacitors, were not changed. The partial layout of the phase shifter is shown in Fig. 1. The unit cell in the new periodic structure is composed of L_{sect1} part and L_{sect2} part. Its equivalent circuit consists of two unequal-length transmission lines connected in series and two identical BST capacitors connected to ground in parallel, as illustrated in Fig. 2, here C_{BST} was labeled with different numbers to differentiate the connection with different transmission lines. It is important to point out that once L_{sect1} part and L_{sect2} part being identical, the new periodic structure will degenerate into a single periodic structure [6]. According

Manuscript received October 17, 2005; revised February 28, 2006.

Q. Meng, X. Zhang, F. Li, J. Huang, X. Zhu, D. Zheng, and Y. He are with the National Laboratory for Superconductivity, Institute of Physics and Beijing National Laboratory for Condensed Matter Physics, Chinese Academy of Sciences, Beijing 100080, China (e-mail: qdmeng@ssc.iphy.ac.cn).

B. Cheng is with the Key Laboratory of Optical Physics, Institute of Physics, Chinese Academy of Sciences Beijing 100080, China.

Q. Luo and C. Gu are with the Laboratory of Microfabrication, Institute of Physics, Chinese Academy of Sciences, Beijing 100080, China.

Digital Object Identifier 10.1109/LMWC.2006.875622

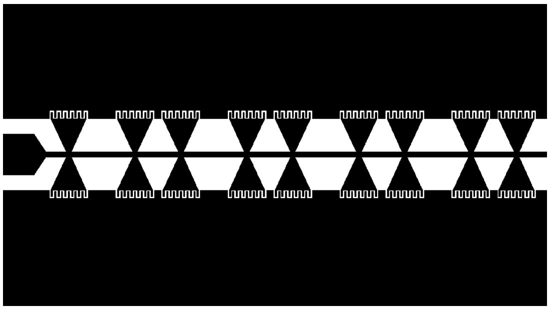

Fig. 1. Photograph of a segment of the phase shifter with new structure.

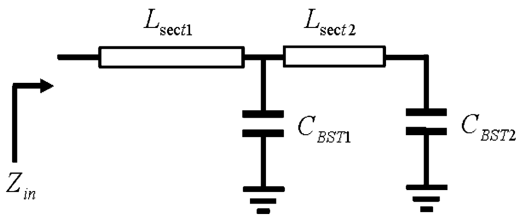

Fig. 2. Equivalent circuit cell for the phase shifter with new structure.

to (2), the obtainable maximal differential phase shift is identical, whatever the simple periodic structure or the new periodic structure was employed.

In the circuit, the dielectric constant of BST thin film is much larger than that of the substrate, so impedance matching is a severe problem. According to the theory about matching network combining series transmission lines and lumped shunt capacitor [7], in a circuit like Fig. 2, the input impedance Z_{in} is a function of the distance between the load (C_{BST2}) and the shunt capacitor (C_{BST1}) location. In other word, once the total length $L_{\sec t1} + L_{\sec t2}$ is kept fixed and the placement of the shunt capacitor C_{BST1} is varied from the beginning of the matching network to the load (C_{BST2}) (i.e., $0 \leq L_{\sec t1} \leq L_{\sec t1} + L_{\sec t2}$), the real and imaginary parts of the input impedance Z_{in} varies with different length of L_{sect1}. This means Z_{in} is a function of the length of L_{sect1}. This type of network has a rather larger tuning capability. So there exists an optimal length of L_{sect1} which makes the input impedance (Z_{in}) match well with the load (C_{BST2}). To apply the above described impedance matching theory to the design of phase shifter, i.e., connecting several matching networks described above in series constitutes the phase shifter with a new structure. Here, C_{BST2} is assumed to be the load. With the given capacitor value, there exists an optimal distance L_{sect1} making the impedance matching of the whole circuit perfect. At this condition, the return loss of the phase shifter should be small enough. In our demonstration phase shifter, the optimal distance L_{sect1} is determined by sonnet's suites, an accurate and reliable high frequency planar electromagnetic simulation software [8].

In order to learn the improvements in the return loss of the phase shifter, and its operation frequency range, computer simulations, employing sonnet's suites, for two phase shifters have been carried out, one with the single periodic structure and the other with the new periodic structure, keeping all the other parameters identical. The simulated results are shown in Fig. 3.

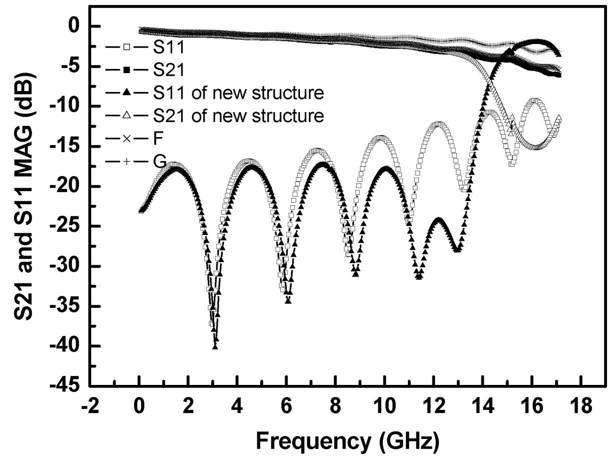

Fig. 3. Simulated S21 and S11 of the phase shifter with different structures. Simulated S21 of the single periodic phase shifter with conductivity of 4.09×10^7 S/m ($- \times -$) and with loss tangents of 0.001 ($- + -$) are also plotted.

Apparently similar to the reported curves [2]–[4], the local return loss maximum of the single periodic phase shifter increases with increasing frequency. For example, the return loss value at 14.2 GHz (-10.8 dB) is 7 dB higher than that at 1.5 GHz (-17.4 dB). At the same time, its insertion loss value decreases with the increasing frequency. Yet in the new periodic structure, the return loss of the phase shifter is almost under -17 dB below the frequency of 13.5 GHz, below which the return loss peaks almost have the same value. It was clearly seen that the impedance matching problem was well solved in this circuit. Furthermore, compared with the single periodic structure, the available frequency range of the phase shifter with new structure is observably extended. Yet, in the single periodic phase shifter, its insertion loss is very large, which comes from the smaller conductivity of the metal layer in the CPW line (set at 2.26×10^7 S/m) and the larger loss tangent (set at 0.05) for the BST thin film. Once the conductivity of the metal layer increases to 4.09×10^7 S/m, or the loss tangent for the BST thin film decreases to 0.001 in the simulation, respectively, its insertion loss will reduce from 2.30 dB to 1.92 dB or 1.37 dB at 9.4 GHz, just as the curve F and G shown in Fig. 3.

III. Device Fabrication and Measurement

In order to verify the above simulation, it is necessary to construct a demonstration phase shifter with the new periodic structure. The phase shifter is fabricated on magnesium oxide (MgO) substrate coated with BST thin film. MgO is chosen as the substrate because it has very good insulating properties and low loss tangent. 3000 Å BST film was deposited on MgO substrate by pulse laser deposition. Then, the BST film was ion milled away except two dozen small patches, which were protected by photoresist and left as interdigital capacitor active regions. After the unwanted BST film being removed, 1.2-μm-thick gold film was sputtered on the top of the wafer as conducting layer. The next procedure was patterning of the CPW structure with a photo-mask similar to that shown in Fig. 1. Following standard processes of etching, dicing, and assembling, a demonstration device was then constructed. The main parameters of the phase shifter are as follows: BST thickness 3000 Å, interdigital

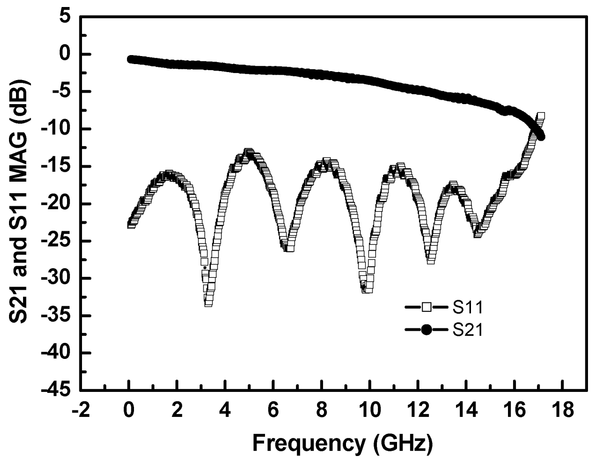

Fig. 4. Measured frequency response of the phase shifter with new structure.

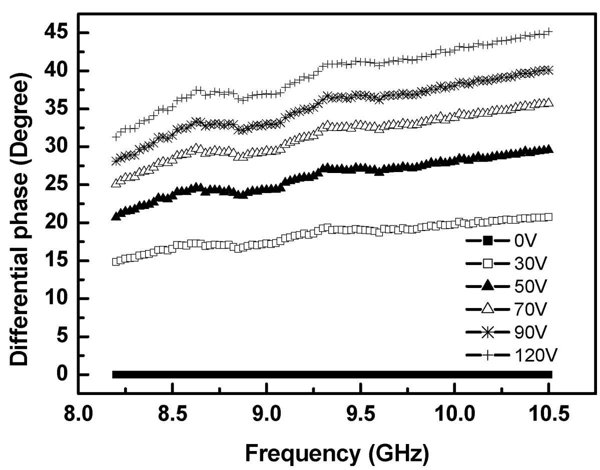

Fig. 5. Differential phase shift at different bias voltages as a function of frequency.

capacitor active region area $460 \times 100\ \mu m^2$, capacitor number 2×12, finger length, width, and spacing 60 μm, 20 μm, and 20 μm, respectively. MgO substrate area, thickness, relative dielectric constant, and loss tangent $5 \times 10\ mm^2$, 500 μm, 9.8 and 1.6×10^{-5}, respectively.

RF measurements were made on an Agilent 8510C network analyzer. The S-parameters of the phase shifter were recorded up to 17.1 GHz for different bias voltages. Fig. 4 shows the transmission loss and return loss of the phase shifter at zero bias, its return loss is almost under -15 dB from dc to 16 GHz, and the return loss peaks almost have the same value, at the frequency range up to 10.5 GHz, its insertion loss is better than -4.2 dB. Apparently the measured results are in good agreement with the results predicted by the computer simulation. The small differences between them come from the fact that both the dielectric constant and loss tangent of the BST thin film used in the simulation are not exactly the same values of the actual BST thin film employed in the phase shifter. The measured differential phase shifts with respect to the zero bias are plotted in Fig. 5, and the insertion losses under different bias voltages are plotted in Fig. 6. At 9.4 GHz, the insertion loss decreases from -3.4 dB to -2.3 dB under 120-V bias voltages. The small ripples in Figs. 5 and 6 come from the local return loss maximum around 8.25 GHz.

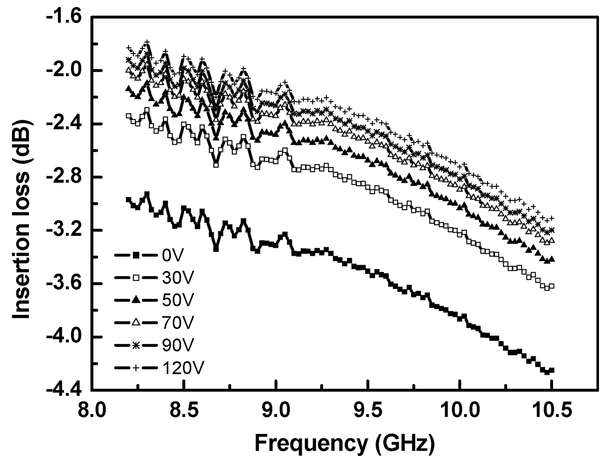

Fig. 6. Different transmission loss at different bias voltages as a function of frequency.

It is worth pointing out that compared with the results of other groups [3]–[5], the figure of merit of this phase shifter is not high enough, which is attributed to the smaller differential phase shift and larger insertion loss. The smaller differential phase shift is due to the lower electric intensity existing between the fingers in the interdigital capacitor for wider fingers spacing, the larger insertion loss mainly determined by CPW transmission line loss, loaded capacitor loss. The 1.2-μm-thick gold layer with conductivity of 2.26×10^7 S/m is quite poor, which contributes much to the loss of the phase shifter. Furthermore, the higher loss tangent of the BST thin film to forming a variable capacitor also brings another considerable contribution to the total loss of the circuit. Once the lower electric intensity located at the fingers spacing is increased, simultaneously, the metallic loss and the loss tangent of BST thin film are reduced in the device fabrication processes, a better performance should be achieved.

REFERENCES

[1] A. Kozyrev, V. Osadchy, A. Pavlov, and L. Sengupta, "Application of ferroelectrics in phase shifter design," in *IEEE MTT-S Dig.*, Jun. 2000, vol. 3, pp. 1355–1358.

[2] F. D. Flaviis, N. G. Alexopoulos, and O. M. Stafsudd, "Planar microwave integrated phase-shifter design with high purity ferroelectric material," *IEEE Trans. Microw. Theory Tech.*, vol. 45, no. 6, pp. 963–969, Jun. 1997.

[3] Y. Liu, A. S. Nagra, E. G. Erker, P. Periaswamy, T. R. Taylor, J. Speck, and R. A. York, "BaSrTiO3 interdigitated capacitors for distributed phase shifter applications," *IEEE Microw. Guided Wave Lett.*, vol. 10, no. 11, pp. 448–450, Nov. 2000.

[4] B. Acikel, T. R. Taylor, P. J. Hansen, J. S. Speck, and R. A. York, "A new high performance phase shifter using BaxSr1 xTiO3 thin films," *IEEE Microw. Guided Wave Lett.*, vol. 12, no. 7, pp. 237–239, Jul. 2002.

[5] E. G. Erker, A. S. Nagra, Y. Liu, P. Periaswamy, T. R. Taylor, J. Speck, and R. A. York, "Monolithic Ka-band phase shifter using voltage tunable BaSrTiO parallel plate capacitors," *IEEE Microw. Guided Wave Lett.*, vol. 10, no. 1, pp. 10–12, Jan. 2000.

[6] A. S. Nagra and R. A. York, "Distributed analog phase shifters with low insertion loss," *IEEE Trans. Microw. Theory Tech.*, vol. 47, no. 9, pp. 1705–1711, Sep. 1999.

[7] R. Ludwig and P. Bretchko, *RF Circuit Design Theory and Application*. Upper Saddle River, NJ: Prentice-Hall, 2002, p. 434.

[8] J. C. Rautio, "Applied numerical electromagnetic analysis for planar high-frequency circuits," in *Encyclopedia of RF and Microwave Design*. New York: Wiley, 2005, pp. 397–413.